Numerical Study on Bilateral Stagger Cantor Fractal Baffles Micromixer

Chen, Xueye*+

College of Transportation, Ludong University, Yantai, Shandong 264025, P.R. CHINA

Lv, Honglin

Faculty of Mechanical Engineering and Automation, Liaoning University of Technology, Jinzhou, Liaoning 121001, P.R. CHINA

ABSTRACT: *Changing the structure of the microchannel or setting obstacles in the microchannel has become an effective way to improve the mixing performance of a passive micromixer. Here, we design a three-dimensional micromixer with fractal obstacles based on Cantor fractal principle. The effect of fractal obstacle level, micromixer height, spacing between fractal obstacles, and different Re (Reynold number) on the mixing efficiency is studied. Some valuable conclusions are obtained. The micromixer with quadratic fractal obstacles has better mixing efficiency than the micromixer with primary fractal obstacles. With the increase of the micromixer height, the effective folding area of the fluid can be increased. When the spacing between the fractal barriers is 0 μm, the mixing efficiency of the micromixer is better. The mixing efficiency of all micromixers can reach more than 90% at Re is less 0.1 or more than 40. When Re is 70 and 100, the fluid convection in the micromixer is very strong. Finally, the best micromixer CSM_{600}(Cantor structure micromixer with height 600μm) is obtained. The mixing effect is superior to other micromixers under any conditions.*

KEYWORDS: *Cantor structure; Fractal obstacle; Mixing efficiency; Numerical simulations.*

INTRODUCTION

With the rapid development of the microfluidic chip, a miniaturized system based on the microfluidic principle is widely used in biochemical, medical, and other fields [1-3]. Because of the small size and velocity, the flow is in a laminar state, which leads to slow lateral diffusion between molecules.[4-6] Therefore, the solution can not mix well in the passive micromixer. There are two principles available for mixing in microchannels based on energy sources. They are active micromixers and passive micromixers. Active micromixers can use external energy sources to mix fluid, can be used to mix fluids, such as pressure field interference [7-8], ultrasonic devices [9], electric field [10], magnetic field [11], etc. Compared with the active micromixer, the passive micromixer does not need any external energy input except for the application velocity or pressure drop at the inlet.

Because of its simple fabrication and operation, passive micromixer has been widely used in many micro devices [12]. Optimizing the structure of microfluidic chips to improve the mixing efficiency of micromixers has become a research hotspot [13-14]. *Bhagat et al.* introduced an obstacle in the microchannel and the flow

* *To whom correspondence should be addressed.*
+ E-mail xueye_chen@126.com
1021-9986/2022/7/2496-2504 9/$/5.09

of the fluid is divided, stretched, and folded [15-17]. In recent years, many research teams have conducted research on passive micromixers. *Stroock et al.* introduced the mode of the rotating flow field on the channel wall, such as a staggered herringbone micromixer [18]. *Schönfeld et al.* The interface area of the fluid is increased exponentially by splitting and reorganizing the fluid repeatedly in horizontal and vertical planes [19]. *Chen et al.* designed two E-type micromixers by numerical analysis [20] and designed a zigzag microchannel by applying an optimization algorithm [21]. *Wang et al.* designed a new micromixer with continuous stratification based on Baker. Because of the stratification effect, the interface area between the two flows increases, so the Baker micromixer has higher mixing efficiency at a low Reynolds number [22]. In addition, the obstacles with the fractal structure are also applied to the design of the micromixer. These obstacles enhance the chaotic convection of the fluid in the microchannel and improve the mixing efficiency [23-24]. *Shah I. et al.* [25] proposed a simple design of a micromixer based on the concept of fractal structure. This fractal structure is composed of mixing units of different shapes and is used for folding and chaotic advection in fluid flow. These designs are made on glass through a 3D multi-head printing system, and the mixing performance is tested experimentally. We compare and analyze the research results of this article with the experimental results and CFD in this paper. Through the research foundation of these research teams, we have made innovations in this. We apply the fractal principle to the field of micromixers.

In this paper, a micromixer with Cantor fractal structure is designed. Since the fractal principle is a very popular and active new theory in the world today, we have reason to believe that its application in micromixers will have a certain impact on the development of this field. So the research of micromixers based on the fractal principle is very necessary. In this work, we analyze the influence of primary fractal and quadratic fractal on the mixing performance of the micromixer. More is to compare the mixing performance of CSMx (Cantor structure micromixer with height x) when Re is 0.01 to 100, and explain the mechanism of mixing enhancement in each type of micromixer. The effects of the height of the microreactor, the distance between the fractal obstacles, and the level of the fractal obstacles on the mixing efficiency are compared. In the end, the optimal micro-mixer CSM600 was obtained.

MODEL DESIGN

Numerical model

The Navier-Stokes equations and the continue equations are usually used to describe the dynamic properties of velocity and pressure for incompressible fluidic flows, its form can be expressed as follows [17]:

$$\rho \cdot \left(\frac{\partial u}{\partial t} + (u \cdot \nabla u) \right) = f - \nabla p + \eta \nabla^2 u \quad (1)$$

$$\nabla \cdot u = 0 \quad (2)$$

Where $\boldsymbol{u}$ represents the velocity vector, f represents the force, ρ represents the density of the fluid, p represents the pressure, η is the dynamic viscosity, t represents the time.

The species transport can be described by the diffusion-convection equation as shown in Equation (3).

$$\frac{\partial c}{\partial t} + (V \cdot \nabla) C = D \nabla^2 C \quad (3)$$

Where C is concentration and D is the diffusion constant of the species.

The variables for the species mixing studies are the flow velocity corresponding to the characteristic dimensionless number *Re*.

$$Re = \frac{u L_c \rho}{\eta} \quad (4)$$

$$L_c = \frac{2HW}{H + W} \quad (5)$$

Where *Re* is the ratio between momentum and viscous friction, L_C indicates the characteristic length of the flow, and η is the dynamic viscosity of the fluid. H is the height. W is the width.

$$M = 1 - \sqrt{\frac{1}{N} \sum_{i=1}^{N} \left(\frac{C_i - \overline{C}}{\overline{C}} \right)^2} \quad (6)$$

Where M is the mixing efficiency of the micromixer, N is the total number of sampling points, and C_i and $\overline{C}$ are normalized concentration and expected normalized concentration, respectively. Mixing efficiency ranges from 0 (0%, not mixing) to 1 (100%, full mixed).

Geometrical model

The geometric structure of the micromixer is mainly to add obstacles in the T-type microchannel. Fig.1 shows the design process of the obstacle. A simple fractal

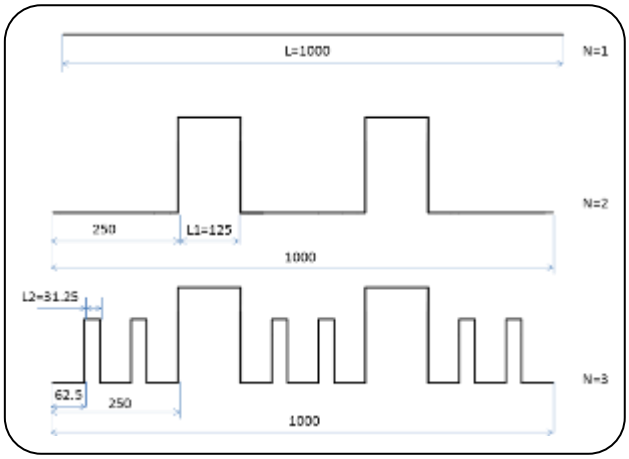

Fig. 1: Fractal process of Cantor structure.

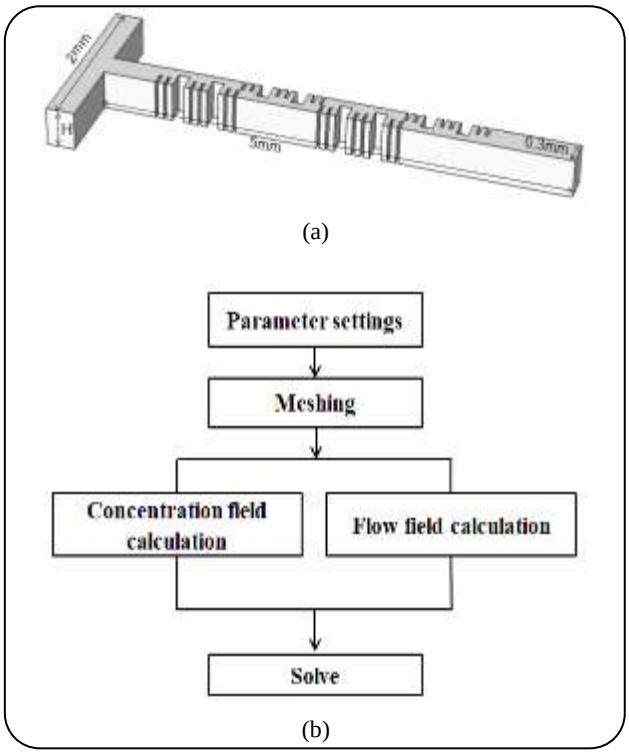

Fig. 2: (a) Cantor structure micromixer with four quadratic obstacles, (b) Flow chart of numerical program.

structure model is designed by Cantor fractal principle. The fractal process is as follows:

(1) Selecting a straight line with a length L=1000μm

(2) Dividing the straight line into eight equal parts L_1 = 1/8 L, L_1 = 125 μm, the primary fractal as shown in Fig.1(N=2).

(3) The rest of the lines are divided in the same proportion L_2 = 1/8 L_1, L_2 = 31.25 μm, the quadratic fractal as shown in Fig.1(N=3).

In the process of modeling the micromixer, we design the size of the micromixer according to the fractal principle and the rationality of the parameters. Combining obstacles with microchannels. Four fractal obstacles are regularly placed in the microchannel. Fig.2(a) shows the micromixer after the combination of microchannels and fractal obstacles. Fig.2(a) is a micromixer with four quadratic obstacles. The main dimensions of the micromixer are shown in the figure. H is the height of the micromixer. Fig. 2(b) shows the solution process.

As shown in Fig. 3, we designed four different grids for research. The final choice is Mesh 3. The statistics of the complete mesh include 216,681 vertices. The number of tetrahedrons is 788860. The number of pyramids is 7656. The number of prisms is 128896. The number of triangle meshes is 71922. The number of quadrilaterals is 240. The number of edge units is 4972. The number of vertex units is 280.

RESULTS AND DISCUSSION

The COMSOL Multiphysics software is a numerical simulation software that is based on the finite element method. It can solve some partial differential equations in the physics simulation. The samples in the model are blue ink and red ink with different concentrations. The concentrations are set to C_1 = 1mol / L and C_2 = 0 mol /L respectively. The diffusion coefficient of dissolved components is 1×10^{-9} m^2 / s. The microchannel inlet is set at a different speed, and the pressure at the outlet is 0 Pa. The fluid dynamic boundary conditions are no-slip at all walls.

Effects of fractal obstacle levels on the mixing efficiency

In this section, the effect of fractal obstacle levels on the efficiency of micromixers is studied. Two micromixers with H=0.6 mm are selected to compare their mixing performance. Their mixing efficiency is compared in Fig.4. As can be seen from Fig.4, the micromixer with quadratic fractal obstacles has better mixing efficiency than the micromixer with primary fractal obstacles. Because when Re = 1, the fluid flow mainly depends on the intermolecular force for diffusion, the mixing efficiency is low. In other Res, chaotic convection is generated and the mixing efficiency is increased. In addition, the minimum mixing efficiency of the micromixer with quadratic fractal obstacles can reach 85%. Therefore, the fractal obstacle level has a great influence on the mixing efficiency.

The effect of micromixer height on the mixing efficiency

In this section, the mixing efficiency of CSM_x(x stands for the micromixer height) is compared. And x are 100μm, 200μm, 400μm and 600μm. Several microchannels are micromixers with quadratic fractal obstacles.

In order to find a better micromixer, the mixing efficiency of four kinds of high micromixers is calculated under different Re. Fig.5 shows the mixing efficiency of CSM_x at different Re. Re ranges from 0.01 to 100. From Fig.4, the volume of the micromixer increases gradually with the increase of the height of the micromixer. This is because when the height of the micromixer increases, the fluid in the channel has more space for mixing, and at the same time, the ability of the fluid to generate chaotic convection is increased. The two different fluids have more contact and diffusion to improve the mixing performance. When x is 600μm, the mixing efficiency of the micromixer is better. The mixing efficiency of all micromixers can reach more than 90% at Re is less 0.1 or more than 40. When the flow velocity is small, the fluid can be fully mixed by molecular diffusion. But with the increase of the flow velocity, the retention time of the fluid in the microchannel is short, which can not be fully mixed by molecular diffusion. When the velocity increases further, the fluid can be mixed by convection. So the curve of mixing efficiency is non-monotonic.

We compare the results in this study with the CFD results of *Shah I. et al.* [25]. The research result of them is that when Re is 0 - 40, the mixing efficiency of the micromixer ranges between 10% and 70%. It can be seen from Fig. 5 that the mixing efficiency of the CSM in this study can reach 60% - 100% between Re=0 - 40. Compared with the study of *Shah I. et al.*, the mixing efficiency of CSM is increased by more than 50%. The mixing performance of CSM in this study almost reached complete mixing. Therefore, the design of the micromixer channel structure in this article is very effective, and it greatly improves the mixing efficiency of the micromixer. Furthermore, it can be proved that the channel structure designed in this research can greatly improve the mixing efficiency, which proves the effectiveness of this work. We compare the concentration profiles with baffles. As shown in Fig. 6, we compare the concentration cross-section diagrams when Re=5, 10, 25, and 50 in this work with the experimental results of *Shah I. et al.* It can be found that as the concentration of Re increases, the surface contact area increases and the diffusion capacity increases, leading to uniform mixing and increasing mixing efficiency.

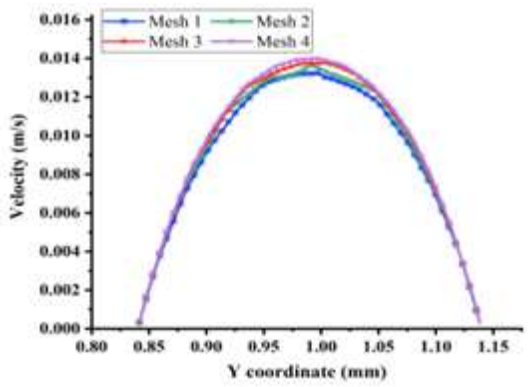

Fig. 3: Grid independence test.

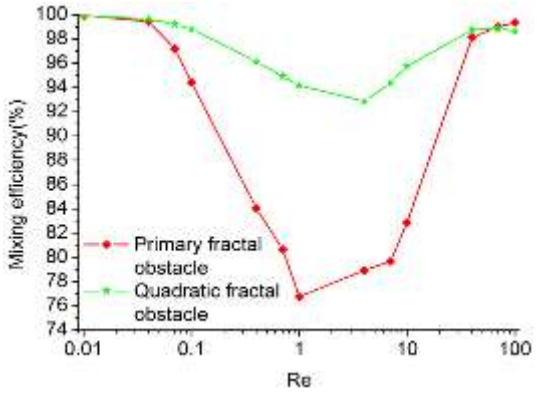

Fig. 4: The mixing efficiency of two micromixer at different Re.

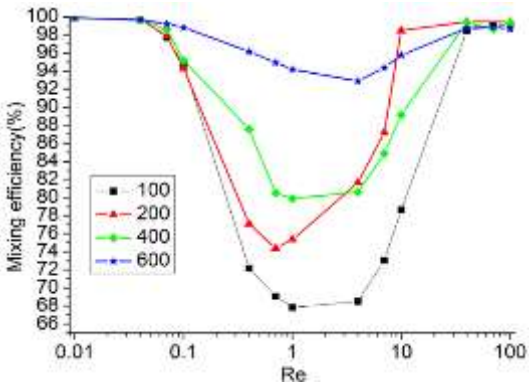

Fig.5: Mixing efficiency of CSMx at different Re.

The effect of spacing between fractal obstacles on the mixing efficiency

Firstly, a micromixer with four quadratic fractal obstacles is selected. Secondly, three kinds of spaces between obstacles are studied. The three spaces are 0μm,

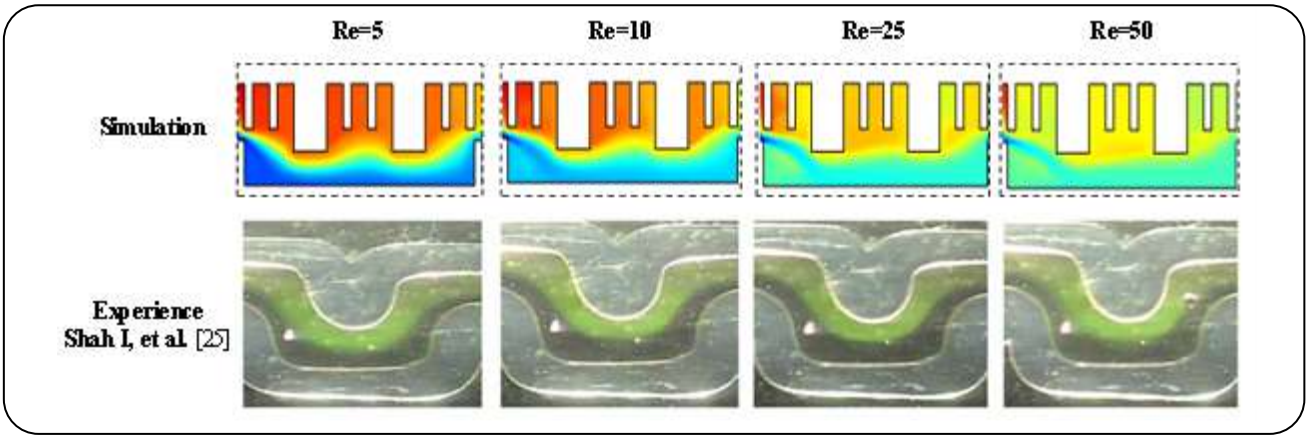

Fig. 6: Contrast between numerical simulation and experimental analysis of Shah I. et al. [25].

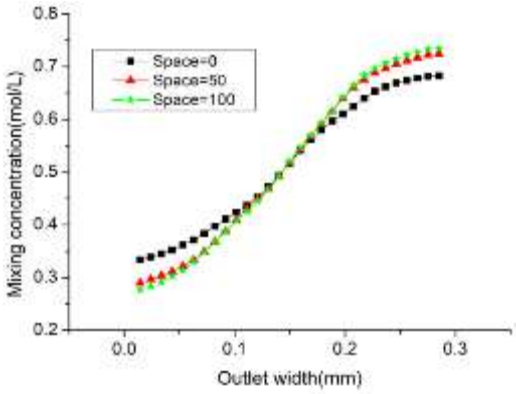

Fig.7: The mixing concentration at the outlet of the micromixer.

50μm and 100μm. Fig.7 shows the mixing concentration at the outlet of the micromixer with different spacing. The ordinate in Fig. 5 represents the concentration change of the micromixer. When the width is 0.15 mm, it is just at the midpoint of the outlet surface of the micromixer. At this time, the concentration is closest to 0.5 mol / L. The level of the curve in this graph does not represent the mixing performance of the micromixer. At 100 μm, the curve is the farthest from the perfect mixing concentration of 0.5 mol / L, so the mixing performance is the worst at this time. At 0 μm, Micromixer has the best mixing performance. Fig.8 shows the local mixing performance of micromixers. Fig.9 shows the color concentration chart at the outlet of the micromixer.

From Fig.7, when the space is 0μm, the mixing performance of the micromixer is better. From Fig.8, the decrease in space makes the fluid mix better. When the fluid passes through a smaller space, which can promote better contact with the fluid. As you can see from Fig.9, the range of the color of the concentration is smaller, which represents a better mix. Thus, the mixing performance of micromixers can be improved by reducing the space between obstacles in microchannels.

The effect of different Re on the mixing efficiency

In this section, we study the nonmonotonicity of mixing efficiency with Re. The mixing phenomenon of Re in the range of 0.01 to 1 and 1 to 100 is analyzed. We choose a micromixer with a height of 100 for research and analysis. As shown in Fig.10, we select a plane in the micromixer to analyze the flow and mixing of the fluid.

Effects of low Re(0.01<Re≦1) on the mixing efficiency

The concentration cross sections under four Re are compared and analyzed. As shown in Fig.11, the direction of the arrow in the plane represents the flow direction, and the color represents the size of the concentration value. As can be seen from the figure, the flow state of the fluid is similar. But the effect of mixing is different. When Re = 0.04, the mixing effect of fluid is better. This is because when the flow velocity of the fluid is small, it stays longer in the micromixer, and the fluid can be better mixed by molecular diffusion. It can be seen from the previous research results that when Re is less than 1, the convection phenomenon of the fluid is very poor. From the results of this study, it can be seen that the fractal obstacle structure makes the flow direction of the fluid deflect obviously at low Re.

Effects of high Re(1<Re≦100) on the mixing efficiency

From Fig.5, the mixing performance of the micromixer is gradually improved with the increase of Re at Re > 1. Therefore, this section will compare the mixing

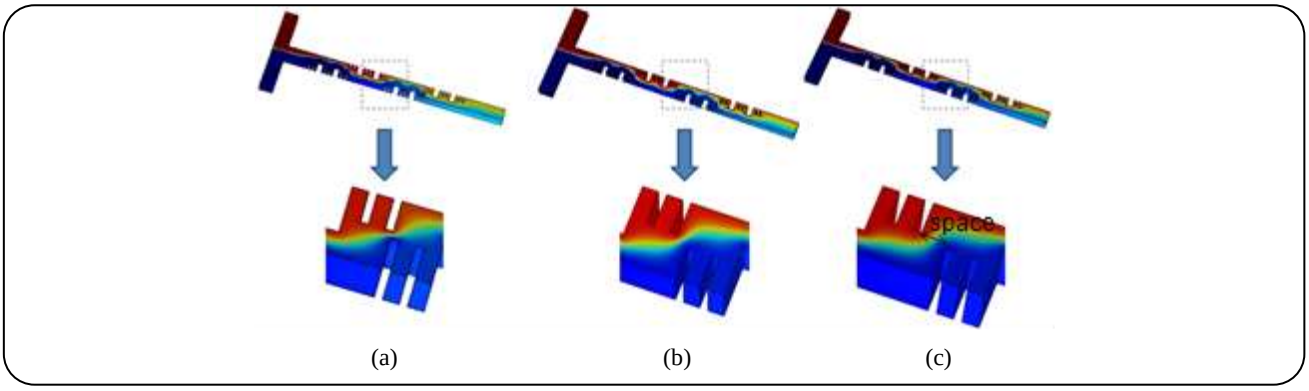

Fig. 8: The mixing performance of micromixers at different spaces (0μm, 50μm, 100μm).

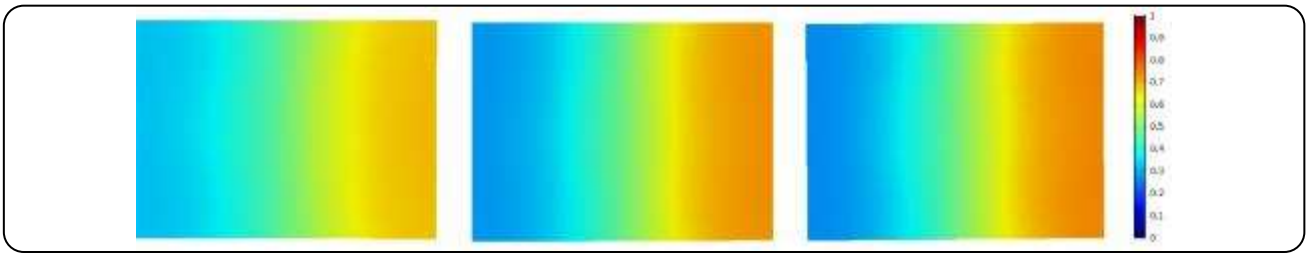

Fig.9: The color concentration chart at outlet of micromixer.

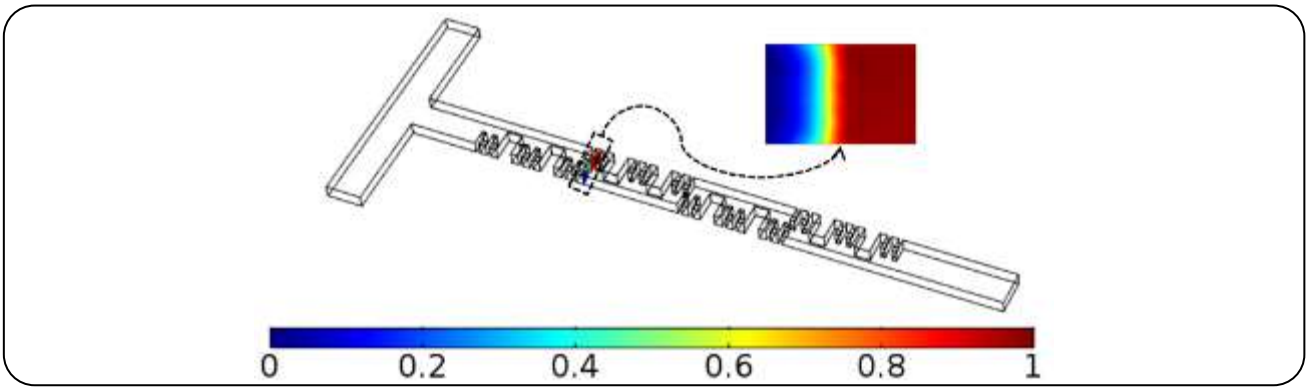

Fig. 10: Selecting an interface in the CSM_{100} at Re=1.

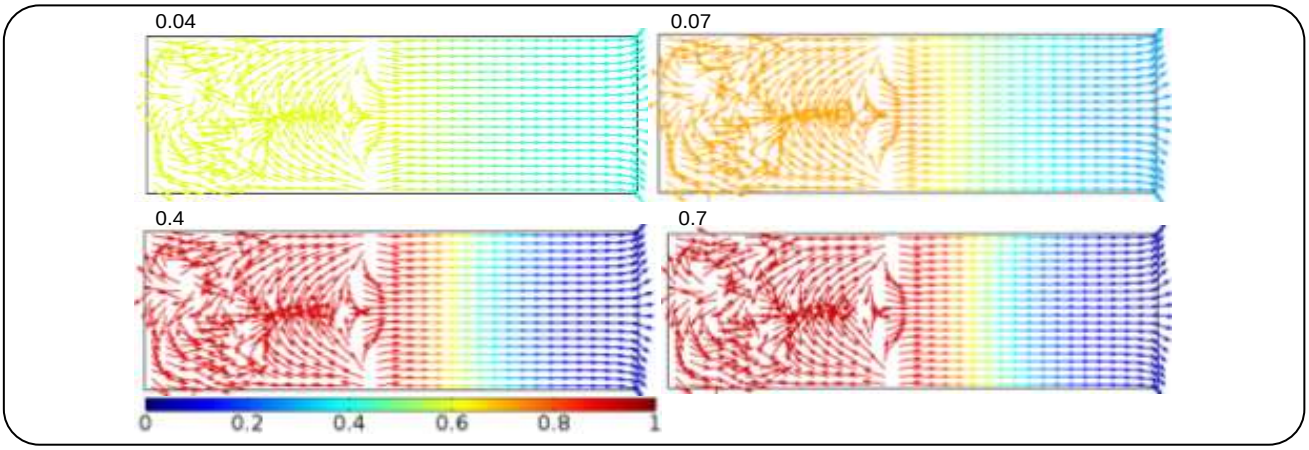

Fig. 11: The concentration planes of CSM_{100} at Re=0.04, 0.07, 0.4 and 0.7.

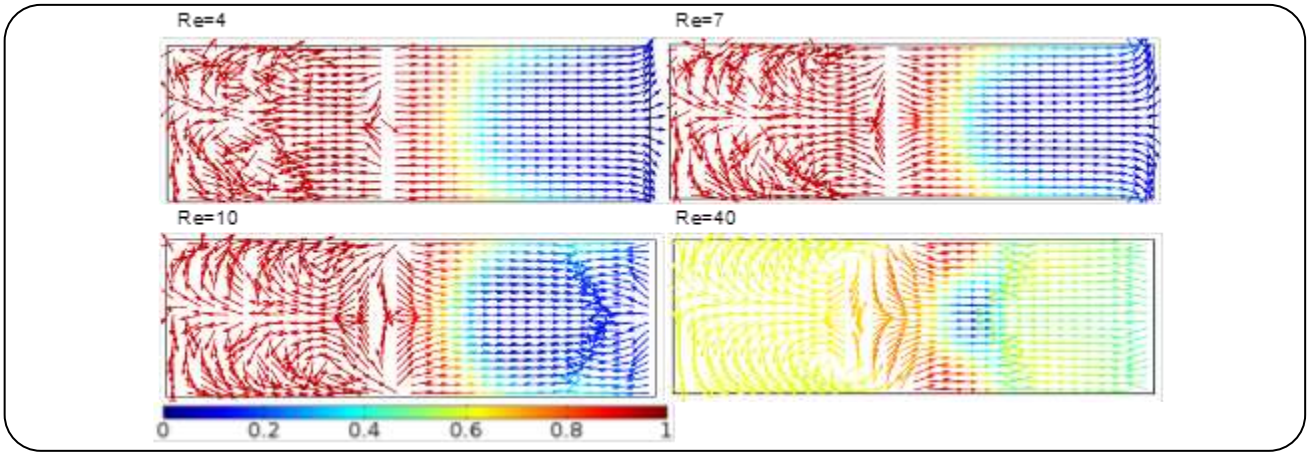

Fig. 12: The concentration planes of CSM_{100} at Re=4, 7, 10 and 40.

performance of CSM_{100} at high Re (1<Re≦100). Fig.12 shows the concentration planes of the CSM_{100} at Re=4, 7, 10, and 40. It can be seen that with the increase of Re, convection gradually dominates. When Re is 4 and 7, the flow of fluid in the microchannel has little difference, which is consistent with the results shown in Fig.7. When Re = 10, the convective phenomenon of the fluid species begins to increase, but the mixing effect has not been significantly enhanced. When Re = 40, the convection is further strengthened, and the mixing effect of the fluid is better. This is because, at higher flow velocity, the obstacle structure causes more intense convection of the fluid.

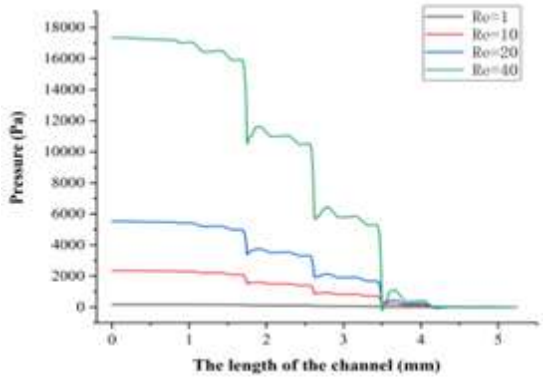

Fig.13: The pressure of CSM_{100} at Re=1, 10, 20 and 40.

Effects of different Re(1<Re≦100) on the pressure

In the end, we study the pressure drop of CSM_{100} at different Res. The pressure drop is also very important as a parameter for evaluating the micromixer. The greater the pressure drop, the lower the safety of the micromixer. Fig. 13 shows the pressure curve of CSM_{100} at Re = 1, 10, 20, and 40. It can be seen that with the increase of Re, the pressure drop of the micromixer also increases. This is because when Re increases, the mixing ability of the fluid in the channel is improved, resulting in chaotic convection. As a result, the reliability of the micromixer decreases and the pressure increases.

CONCLUSIONS

In this paper, a high-efficiency three-dimensional passive micromixer with Cantor fractal structure is designed. Through the above numerical simulation, some conclusions can be obtained.

(i) The mixing efficiency of the micromixer is affected by the increase of fractal obstacle level and the folding of the fluid in the mixture. The micromixer of quadratic fractal obstacles has better mixing efficiency. The minimum mixing efficiency of the quadratic fractal micromixer, such as CSM_{600}, can reach 85%.

(ii) As micromixer height increases, the mixing efficiency can be improved. When $_{X=}$600μm, the mixing efficiency of the micromixer is the best. Even if Re=1, the mixing efficiency of the CSM_{600} is still higher. When the Re is less than 0. 1 or more than 70, the four micromixers have higher mixing efficiency, all of which are above 94%. However, when Re is between 1 and 70, the mixing efficiency increases with the increase of the micromixer height.

(iii) The mixing performance can be improved by reducing the spacing between adjacent fractal obstacles in the microchannel. In this paper, when the spacing

between adjacent fractal obstacles is 0μm, the mixing efficiency is higher.

(iv) At low Re, the molecular diffusion limits the mixing of fluids, and mixing efficiency decreases with the increase of Re. At high Re, with the increase of Re, the convection phenomenon is more obvious. When Re>10, the mixing performance increases with the increase of Re.

Through research, it is found that the pressure drop will increase a lot when the mixing efficiency of the micromixer is high. This leads to a decrease in the safety of the micromixer. The higher the pressure drop, the higher the pressure at the inlet of the micromixer. At this time, the reliability of the micromixer is lower. Therefore, it is very important to find a micromixer with low mixing efficiency and high pressure in our future research.

Acknowledgment

This work was supported by Young Taishan Scholars Program of Shandong Province of China (tsqn2020), Shandong Provincial Natural Science Foundation (ZR2021JQ).

Received : Apr. 4, 2021 ; Accepted : Aug. 23, 2021

REFERENCES

[1] Ahmadi N., Rezazadeh S., Asgharikia M., Shabahangnia E., Optimization of Polymer Electrolyte Membrane Fuel Cell Performance by Geometrical Changes, *Iran. J. Chem. Chem. Eng. (IJCCE)*, **36(2)**: 89-106 (2017).

[2] Samanipour H., Ahmadi N., Jabbary A., Effects of Applying Brand-New Designs on the Performance of PEM Fuel Cell and Water Flooding Phenomena. *Iran. J. Chem. Chem. Eng. (IJCCE)*, **41(2)**: 618-634 (2020).

[3] Ahmadi N., Rostami S., Enhancing the Performance of Polymer Electrolyte Membrane Fuel Cell by Optimizing the Operating Parameter, *Journal of the Brazilian Society of Mechanical Sciences and Engineering*, **41(5)**: 1-19 (2019).

[4] Rahimi M., Aghel B., Hatamifar B., Akbari M., Alsairafi A., CFD Modeling of Mixing Intensification Assisted with Ultrasound Wave in a T-Type Microreactor, *Chemical Engineering and Processing: Process Intensification*, **86**: 36-46 (2014).

[5] Almasi F., Shadloo M.S., Hadjadj A., Ozbulut M., Tofighi N., Yildiz M., Numerical simulations of Multi-Phase Electro-Hydrodynamics Flows Using a Simple Incompressible Smoothed Particle Hydrodynamics Method, *Computers & Mathematics with Applications*, **81**: 772-785 (2019).

[6] Piquet A., Zebiri B., Hadjadj A., Shadloo M.S., A Parallel High-Order Compressible Flows Solver with Domain Decomposition Method in the Generalized Curvilinear Coordinates System, *International Journal of Numerical Methods for Heat & Fluid Flow*, **30(1)**: 2-38 (2019).

[7] Rahimi M., Aghel B., Alsairafi A.A., Experimental and CFD Studies on Using Coil Wire Insert in a Proton Exchange Membrane Fuel Cell, *Chemical Engineering and Processing: Process Intensification*, **49(7)**: 689-696 (2010).

[8] Shenoy D.V., Shadloo M.S., Peixinho J., Hadjadj A., Direct Numerical Simulations of Laminar and Transitional Flows in Diverging Pipes, *International Journal of Numerical Methods for Heat & Fluid Flow*, **30(1)**: 75- 92 (2019).

[9] Lv H., Chen X., Zeng X., Optimization of Micromixer with Cantor Fractal Baffle Based on Simulated Annealing Algorithm, *Chaos, Solitons & Fractals*, **148**: 111048 (2021).

[10] Gidde R.R., Pawar P.M., Ronge B.P., Misal N.D., Kapurkar R.B., Parkhe A.K., Evaluation of the Mixing Performance in a Planar Passive Micromixer with Circular and Square Mixing Chambers, *Microsystem Technologies*, **24(6)**: 2599-2610 (2018).

[11] Chen X., Zhao Z., Numerical Investigation on Layout Optimization of Obstacles in a Three-Dimensional Passive Micromixer, *Analytica Chimica Acta*, **964**: 142-149 (2017).

[12] Shi X., Huang S., Wang L., Li F., Numerical Analysis of Passive Micromixer with Novel Obstacle Design, *Journal of Dispersion Science and Technology*, **42(3)**: 440-456 (2021).

[13] Zhao S., Chen C., Zhu P., Xia H., Shi J., Yan F., Shen R., Passive Micromixer Platform for Size-and Shape-Controllable Preparation of Ultrafine HNS, *Industrial & Engineering Chemistry Research*, **58(36)**: 16709-16718 (2019).

[14] Bayareh M., Ashani M.N., Usefian A., Active and Passive Micromixers: A Comprehensive Review, *Chemical Engineering and Processing-Process Intensification*, **147**: 107771 (2020).

[15] Jothimuthu P., Bhagat A.A.S., Papautsky I., "PhotoPDMS: Photodefinable PDMS for Rapid Prototyping", *In 2008 17th Biennial University/ Government/Industry Micro/Nano Symposium* (pp. 183-186). IEEE. (2008).

[16] Raza W., Hossain S., Kim K.Y., A Review of Passive Micromixers with a Comparative Analysis, *Micromachines*, **11(5)**: 455 (2020).

[17] Ruijin W., Beiqi L., Dongdong S., Zefei Z., Investigation on the Splitting-Merging Passive Micromixer Based on Baker's Transformation, *Sensors and Actuators B: Chemical*, **249**: 395-404 (2017).

[18] Okazaki Y., Furuno M., Kasukawa T., Adachi J., Bono H., Kondo S., ... & Hayashizaki Y., Analysis of the Mouse Transcriptome Based on Functional Annotation of 60,770 Full-Length cDNAs, *Nature*, **420(6915)**: 563-573 (2002).

[19] Schönfeld F., Hessel V., Hofmann C., An Optimised Split-and-Recombine Micro-Mixer with Uniform 'Chaotic'mixing, *Lab on a Chip*, **4(1)**: 65-69 (2004).

[20] Haghighinia A., Movahedirad S., Mass Transfer in a Novel Passive Micro-Mixer: Flow Tortuosity Effects, Analytica Chimica Acta, **1098**: 75-85 (2020).

[21] Chen X., Li T., A Novel Passive Micromixer Designed by Applying an Optimization Algorithm to the Zigzag Microchannel, *Chemical Engineering Journal*, **313**: 1406-1414 (2017).

[22] Yue L., Junqin H., Shengzhi Q., Ruijin W., "Big Data Model of Security Sharing Based on Blockchain", In *2017 3rd International Conference on Big Data Computing and Communications (BIGCOM)* (pp. 117-121). IEEE. (2017).

[23] Kim C.K., Yoon J.Y., Optimal Design of Groove Shape on Passive Micromixer Using Design of Experiment Technique, *Proceedings of the Institution of Mechanical Engineers, Part E: Journal of Process Mechanical Engineering*, **231(4)**: 880-887 (2017).

[24] Wu Z., Chen X., A Novel Design for 3D Passive Micromixer Based on Cantor Fractal Structure, *Microsystem Technologies*, **25(1)**: 225-236 (2019).

[25] Shah I., Aziz S., Soomro A.M., Kim K., Kim S.W., Choi K.H., Numerical and Experimental Investigation of Y-Shaped Micromixers with Mixing Units Based on Cantor Fractal Structure for Biodiesel Applications, *Microsystem Technologies*, **27(5)**: 2203-2216 (2021).